Dosage-dependent requirement of BMP type II receptor for maintenance of vascular integrity

Dong Liu,[1] Jian Wang,[1] Bernd Kinzel,[2] Matthias Müeller,[2] Xiaohong Mao,[1] Reginald Valdez,[1] Yongxing Liu,[1] and En Li[3]

[1]Developmental and Molecular Pathways, Novartis Institutes for Biomedical Research, Cambridge, MA; [2]Developmental and Molecular Pathways, Novartis Institutes for Biomedical Research, Basel, Switzerland; and [3]Models of Disease Center, Novartis Institutes for Biomedical Research, Cambridge, MA

Germ-line mutations in bone morphogenic protein type II receptor *(Bmpr2)* confer susceptibility to pulmonary arterial hypertension (PAH), which is characterized by obstructive vascular lesions in small arteries. The molecular and cellular mechanisms that account for the etiology of this disorder remain elusive, as does the role of *Bmpr2* in postnatal tissue homeostasis. Here we show that in adult mice, stably silencing *Bmpr2* expression by RNA interference does not increase pulmonary arterial resistance but results in severe mucosal hemorrhage, incomplete mural cell coverage on vessel walls, and gastrointestinal hyperplasia. We present evidence that BMP receptor signaling regulates vascular remodeling during angiogenesis by maintaining the expression of endothelial guidance molecules that promote vessel patterning and maturation and by counteracting growth factor–induced AKT activation. Attenuation of this function may cause vascular dysmorphogenesis and predisposition to angioproliferative diseases. Our findings provide a mechanistic link between PAH and other diseases associated with the BMP/TGF-β pathways, such as hereditary hemorrhagic telangiectasia and juvenile polyposis syndrome. (Blood. 2007;110:1502-1510)

Introduction

The bone morphogenic proteins (BMPs) regulate a variety of developmental processes, including angiogenesis. According to the current model, each BMP binds to a type II receptor (BMPR2, ACVR2A, or ACVR2B) and recruits a type I receptor (BMPR1A, BMPR1B or ACVR1). Upon receptor activation, the SMAD proteins, including SMAD1, SMAD5, and SMAD8, act as intracellular signal transducers by translocating to the nucleus and regulating transcription.[1] Exogenously added BMPs have been shown to modulate vasculogenesis or angiogenesis in cell culture models[2] and tumor xenografts.[3] Genetic evidence further implicated BMP signaling in cardiovascular development. *Bmp4*-deficient mouse embryos display reduced number of blood islands, possibly due to a defect in endothelial progenitor differentiation.[4] Likewise, *Smad5*-null mice are able to form a primitive vascular plexus but fail to establish a mature vascular network.[5,6] Moreover, mice lacking ALK1 or endoglin, components of an endothelium-restricted TGF-β receptor complex capable of signaling through the BMP SMADs, exhibit excessive fusion of capillary plexus and vessel hyperdilation.[7-9] However, the early lethality and the complexity of the embryonic phenotype prevent precise delineation of the underlying molecular mechanisms. More recently, specific roles of BMP signaling in the circulatory system have been demonstrated by inactivating *Bmpr1a* in FLK1-expressing mesoderm, which gives rise to smooth-muscle, endothelial, and hematopoietic cells.[10] The conditional knockout mice survive until midgestation and exhibit multiple abnormalities in vessel remodeling and maturation. Despite such revelation, novel strategies are needed to gain insight into the function of this pathway during later stages of organ development and postnatal homeostasis.

The significance of such function is evident in human vascular disorders. Haploinsufficiency of *Bmpr2* and *Alk1* underlies the pathogenesis of pulmonary arterial hypertension (PAH) and hereditary hemorrhagic telangiectasia (HHT), respectively.[11-13] PAH is characterized by abnormal proliferation of endothelial and smooth muscle cells, which leads to progressive occlusion of the small pulmonary arteries and persistent elevation of vascular resistance, whereas HHT is characterized by multisystem vascular dysplasia and arteriovenous malformation. The cellular compartment directly responsible for the onset of abnormal vessel remodeling and the contribution of *Bmpr2* mutations to the pathogenesis of PAH remain obscure. Nonetheless, recent identification of HHT patients with clinical features indistinguishable from those of PAH[14] points to common pathways disrupted by mutations of *Alk1* and *Bmpr2* in inherited pulmonary vascular diseases, thus implicating endothelial dysfunction and aberrant remodeling as a critical but largely unexplored cause in the disease development.

To better understand the role of BMP signaling in maintaining a healthy vasculature, we generated mice expressing short hairpin RNA (shRNA) from a defined genomic locus. This approach resulted in efficient knockdown (KD) of *Bmpr2* expression but otherwise maintained a basal level of function to circumvent the embryonic lethality of the null mutation.[15] Our analyses of these mice suggest that suppressing BMPR2-mediated signaling impinges upon vessel integrity and stability, which may be implicated in the pathogenesis of PAH and related diseases.

Submitted November 20, 2006; accepted May 8, 2007. Prepublished online as *Blood* First Edition paper, May 11, 2007; DOI 10.1182/blood-2006-11-058594.

The online version of this article contains a data supplement.

The publication costs of this article were defrayed in part by page charge payment. Therefore, and solely to indicate this fact, this article is hereby marked "advertisement" in accordance with 18 USC section 1734.

Materials and methods

Generating shRNA-expressing mice

To prepare for site-specific insertion of the shRNA transgene, a conventional targeting vector was designed to allow for recombination-mediated cassette exchange (RMCE) at the *Rosa26* locus. A transcription stop signal was inserted between the 2 homologous arms to prevent read-through of the endogenous mRNA, which is flanked by lox511 and loxP sites in inverse orientation. We obtained recombinant embryonic stem (ES) cell clones containing the modified *Rosa26* locus (Figure 1) through homologous recombination. The exchange vector carried an shRNA expression cassette, consisting of a U6 PolIII promoter upstream of an shRNA duplex: ttggaaaccatcccacat(sense)GTTC-ATGAGA(loop)atgtgggatggtttccaac(antisense)TTTTTT(termination), corresponding to a 19-mer within exon 10 of *Bmpr2*. The entire U6-shRNA cassette, followed by a neomycin selection marker, was flanked by lox511 and loxP sites to allow for RMCE between the exchange vector and modified *Rosa26* acceptor allele. We initially verified the potency of the selected shRNA by stable transfection of the exchange vector in NIH3T3 cells. RMCE was then achieved in 129V ES cells cotransfected with the circular exchange vector and a Cre-expressing plasmid and facilitated by G418 selection. Individual ES clones incorporated with a single copy of the exchanged shRNA cassette was then microinjected into C57BL/6J blastocysts to generate chimera and, subsequently, F1 mice using standard techniques. Unless specified, analyses were carried out when the phenotype became apparent, using F1 hybrid or F2N1 mice that were backcrossed once to C57BL/6J strain. Homozygous mice carrying 2 copies of the shRNA were bred by heterozygote intercrossing. Data shown in this report represent transgene R26C, although we obtained similar results from mouse lines corresponding to both shRNA hairpins. All animal procedures were approved by the Animal Care and Use Committee at Novartis Institutes for Biomedical Research.

Histopathology, immunohistochemistry, and immunoblotting

Tissues were fixed in 10% neutral-buffered formalin and processed for 5-μm paraffin sections. The airway and pulmonary vessels were perfusion fixed. To assess vascular wall thickness, the elastic laminar was highlighted with elastin—Van Gieson staining (Sigma, St. Louis, MO). Fifty randomly selected terminal and respiratory bronchiole-associated pulmonary arteries in the sections—less than 100 μm in diameter—were assessed for their wall thickness and external diameter. Other histologic specimens were stained with hematoxylin and eosin (H&E). Tissues were visualized with an Axio Imager A1 microscope (Carl Zeiss, Thornwood, NY) under Plan-Apochromat (10×/0.45 NA, 20×/0.8 NA, 40×/0.95 NA) objective lenses. Images were acquired using Zeiss AxioCam MRc5 equipped with AxioVision 4.0. The antibodies used in immunohistochemistry included mouse monoclonal anti–smooth muscle α-actin (Sigma), rabbit polyclonal anti–von Willebrand factor (VWF) (Abcam, Cambridge, MA), and rabbit polyclonal anti-Ki67 (DAKO, Cambridge, United Kingdom). Immunoblotting analyses on PVDF membranes were carried out for tissue homogenates or cell lysates in radioimmunoprecipitation assay (RIPA) buffer containing protease inhibitors with antibodies against the following antigens: AKT, pSer473-AKT, PDGFRβ, p-PDGFRβ Tyr751, SMAD2, p-SMAD2, and p-SMAD1,5,8 (Cell Signaling Technology, Danvers, MA), SMAD1 and integrin β1 (Santa Cruz, Santa Cruz, CA), BMPR2 (BD Biosciences, San Jose, CA), pSer785-integrin β1 (Invitrogen, Carlsbad, CA), SEMA3C (R&D Systems, Minneapolis, MN), β-actin, and α-tubulin (Sigma).

Hemodynamics measurements

Three-month-old mice were anesthetized intraperitoneally with a mixture of ketamine (100 mg/kg) and xylazine (10 mg/kg) and positively ventilated with oxygen. For measurement of right ventricular pressure, the right jugular vein was surgically exposed, and a microtip pressure transducer catheter (1.4 French; Millar Instruments, Houston, TX) was inserted via the jugular vein. The catheter was gently advanced into the right ventricle and the pressure/volume data continuously recorded using PowerLab software (AD Instruments). Measurement of left ventricular pressure was carried out subsequently by catheterization of the carotid artery.

Isolation and culture of mouse lung endothelial cells

Cells were isolated from mice 8 to 20 weeks of age. The pulmonary circulation was perfused with PBS before lungs were removed aseptically, minced with sterile scalpels, and digested with 1 mg/mL collagenase and 2 μg/mL dispase II (Roche) for 40 minutes at 37°C. The cell digest was filtered through 70-μm cell strainer and seeded on gelatin-coated dishes in endothelial growth medium (Delbecco modified Eagle medium (DMEM) supplemented with 20% fetal boving serum (FBS), 100 μg/mL endothelial cell (EC) growth supplement (Sigma), 10 U/mL Na-heparin, and 1% penicillin/streptomycin). Two days later, cells were labeled with 10 μg/mL DiO-Ac-LDL (Biomedical Technologies, Stoughton, MA) and PE-antimouse CD45 (BD Pharmingen, Santa Cruz, CA), and the Ac-LDL$^+$CD45$^-$ population was recovered by fluorescent-activated cell sorting (FACS). Cells were maintained in the growth medium and used between passage 3 and 4. To obtain cells used in gene expression analyses, collagenase-digested cell suspension was labeled with Alexaflor-antimouse CD102 (BD) and PE-antimouse CD45 without initial culturing and then subjected to FACS. RNA was prepared from the CD102$^+$CD45$^-$ population. The purity of the ECs was consistently more than 95% as verified by DiO-Ac-LDL uptake and anti-VWF staining.

Cell migration assay

Chemotactic cell migration assays were performed using transwell culture inserts with polycarbonate membranes and 8-μm pore size (Corning). A total of 2×10^5 endothelial cells were serum-starved overnight before being resuspended in the gelatin-coated top chamber containing endothelial basal medium (EBM) (Cambrex, Walkersville, MD) with 0.5% bovine serum albumin (BSA) and treated with 200 ng/mL BMP4 or vehicle control for 3 hours. The inserts were placed in the medium with 0.5% BSA or supplemented with growth factors. Cells were incubated at 37°C for 6 hours. Nonmigratory cells on the upper membrane surface were scraped with a cotton swab, and cells attached to the bottom surface were stained with crystal violet. The average number of migrated cells from 6×200 microscopic fields was counted. Recombinant BMPs used in this study were purchased from R&D Systems.

Matrigel plug assay

Characterization of angiogenesis by morphometric analyses of Matrigel plugs was performed following the criteria established previously.[22] Briefly, 500 μL of liquid Matrigel containing 200 ng/mL basic fibroblast growth factor (bFGF; R&D Systems) and 10 U/mL heparin, with or without 200 ng/mL BMP4, was implanted subcutaneously into each flank of the abdominal area of approximately 10-week-old mice. After 7 days, the plugs were fixed, cut at midline, and processed for histologic analyses of microvessels.

Gene-expression analyses

Total RNA was prepared using RNeasy mini (Qiagen, San Diego, CA). Generation of biotinylated cRNA probe was carried out essentially as described in the standard Affymetrix (Santa Clara, CA) GeneChip protocol. Each sample was hybridized with a Mouse Genome 430 2.0 microarray. Data were normalized by MAS5 algorism using Bioconductor. We applied filters to identify genes associated with the *Bmpr2*-deficient phenotype. First, we used data quality flag restriction, retaining genes as present in all triplicate samples and with signal intensity above a marginal threshold. Second, we carried out variance analyses to filter out genes showing differences with low statistical significance between the control and *Bmpr2* KD group. Comparisons were performed using successive parametric *t* tests and paired *t* tests, with the significance level set at .05. Finally, genes that exhibited 1.5-fold or more change in expression between the 2 groups were retained. A total of 272 of more than 39 000 transcripts represented on the 430 2.0 chip passed the filter constraints. We then carried out hierarchical clustering to visualize genes differentially expressed in the *Bmpr2*-deficient sample.

Expression of selected genes was independently verified by quantitative reverse transcriptase–polymerase chain reaction (RT-PCR) using Taqman Low Density Array or Taqman Assay-On-Demand (Applied Biosystems, Foster City, CA) following the manufacturer's protocols. The relative expression levels were quantified using *Hprt1* as internal control.

Statistics

We determined differences between groups using Student *t* test and 1-way analysis of variance (ANOVA). A value of *P* less than .05 indicated a significant difference. All data are expressed as means plus or minus a standard deviation (SD).

Results

Silencing *Bmpr2* in mice

To investigate the consequence of constitutively attenuated activity of *Bmpr2* in vivo, we designed a *Bmpr2*-specific shRNA transgene under the control of the U6 PolIII promoter. A single copy of the U6-shRNA expression cassette was inserted into an inactivated *Rosa26* locus through RMCE in ES cells (Figure 1A). This strategy allows for high-efficiency incorporation of the transgene while minimizing the positional effect on expression levels commonly associated with conventional random integration transgenic approaches. In contrast to the embryonic lethality caused by the *Bmpr2*-null mutation, F1 mice that transmitted the U6-shRNA minigene were viable and born without gross abnormality. Quantification of the *Bmpr2* mRNA and protein in adult tissues confirmed highly effective RNAi in hemizygous shRNA knock-in mice, with up to 90% reduction in target expression compared with wild-type (WT) littermates (Figure 1B,C). We produced 2 transgenic lines, each expressing an independent shRNA hairpin targeting *Bmpr2* that produced similar gene silencing efficacy and phenotype. For clarity, here we describe the analyses of one of these mouse lines.

Age-dependent mucocutaneous vascular lesions in *Bmpr2* knockdown mice

At birth, the *Bmpr2* knockdown (KD) mice appeared indistinguishable from WT littermates. Over time, however, they all became anemic as evidenced by pallor, dyspnea, and wasting. Upon necropsy, massive intestinal hemorrhage was found, predominantly within the cecum or at the ileocecal junction (Figure 2A). Blood samples from the affected mice showed decreased red cell numbers and vastly expanded reticulocytes, whereas white cell and platelet counts were within reference ranges (data not shown). Furthermore, bone marrow morphology was normal, and no disruption of coagulation function was apparent (data not shown), indicating that the hemorrhage was not due to hematopoietic defects or abnormal clotting. Histologic examination of the ileum and ascending colon of the moribund mice revealed angiodysplasia-like lesions. These manifested as hemorrhage of capillaries and thin-walled small vascular channels in the mucosa (Figure 2B). In addition to the gastrointestinal (GI) tract, vascular lesions were observed in the nail beds, exhibiting a reddened appearance, although these changes occurred in less than 10% of the *Bmpr2* KD mice studied (Figure 2C). The earliest detection of occult fecal blood in *Bmpr2* KD mice was variable, with a male bias in younger animals. Such recurrent, chronic blood loss progressively deteriorated to reach a crisis stage, when the affected mice succumbed to complications of severe microcytic anemia. The anemic *Bmpr2* KD mice developed splenomegaly, with disruption of the spleen follicle structure, and extramedullary hematopoiesis (Figure 2D).

To determine the effect of a declining gene dosage series, we bred mice carrying 2 copies of the U6-shRNA transgene by heterozygote intercrossing. A more severe phenotype was observed in these mice, as demonstrated by an earlier onset of hemorrhage that extended to the upper intestinal tract and stomach. They also exhibited shortened life span, which correlated with the further

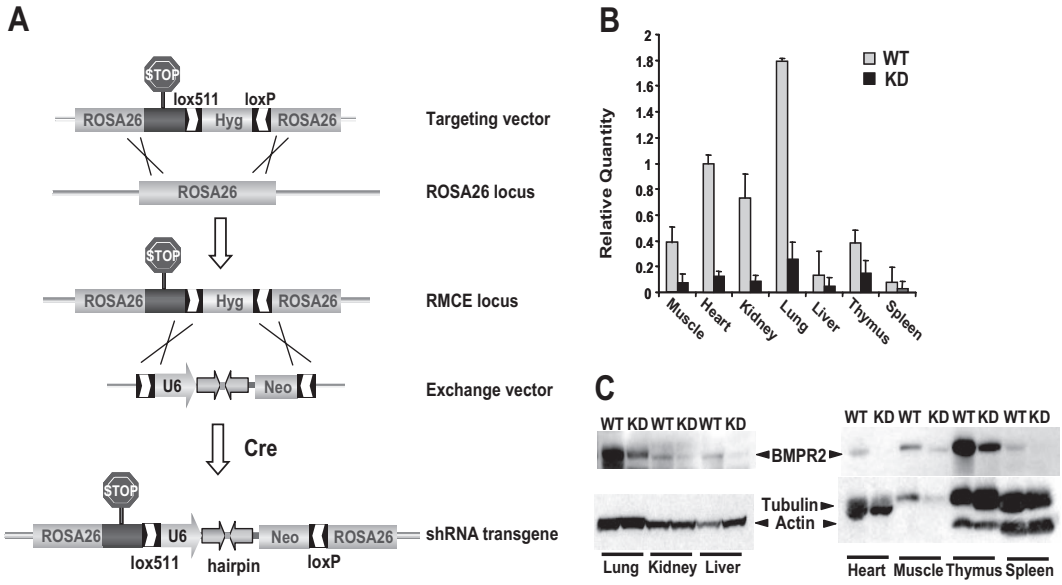

Figure 1. Genetic ablation of BMPR2 function in mice. (A) Ubiquitous expression of shRNA transgene at a defined site in the mouse genome. A modified *Rosa26* locus was generated to allow Cre-mediated RMCE through the heterotypic loxP and lox511 sequences inserted into the locus by gene targeting. Next, homologous recombination in ES cells between the lox sites in the exchange vector and the modified *Rosa26* RMCE locus led to integration of the U6-shRNA expression cassette. (B) In vivo RNA interference. *Bmpr2* mRNA expression in various tissues from wild-type (WT) littermates or *Bmpr2* knockdown (KD) mice was assessed by real-time quantitative PCR. Values are means plus or minus SD. (C) Knockdown of BMPR2 protein expression. BMPR2 was detected in immunoblots of tissue extracts. β-actin and α-tubulin in the same blots serve as internal control.

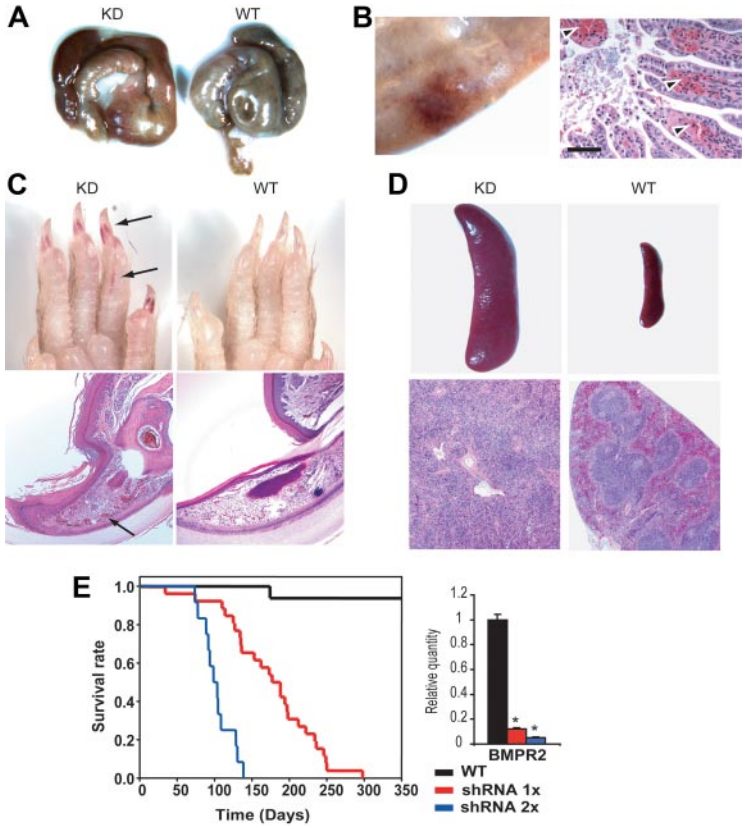

Figure 2. Gross phenotype of *Bmpr2*-deficient mice. (A) Massive bleeding in the cecum. Tissues from a WT littermate are shown in comparison. (B) H&E-stained sections (right) of a segment of ileum (left) from a *Bmpr2* KD mouse. Arrowheads indicate extravasated erythrocytes in the lamina propria. (C) Vascular lesions in the cutaneous extremities. The lesions appeared as redness under the nail bed and dilated capillaries in the histology sections (arrows). Wild-type tissue is shown in comparison. (D) Enlarged spleen as a result of regenerative response to anemia in *Bmpr2* KD mice. The follicles were disorganized, and there were clear signs of extramedullary hematopoiesis. See "Materials and methods, Histopathology, immunohistochemistry, and immunoblotting" for detailed image acquisition information. (E) Survival curves of mice hemizygous (shRNA 1×) or homozygous for the shRNA transgene (shRNA 2×). The bar graph represents the relative *Bmpr2* mRNA expression in the lung of mice with either one of 2 copies of the shRNA transgene, as determined by RT-PCR. Values are means plus or minus SD. $*P < .01$.

diminished levels of *Bmpr2* expression in the lung (Figure 2E). Because unchallenged heterozygous null mutants are spared of major vascular phenotype,[15] we conclude that a critical level of signaling strength from the BMP receptor is required to maintain vascular integrity in adult animals.

GI hyperplasia concomitant with vascular lesions in *Bmpr2* knockdown mice

Over time, GI polyposis developed in many *Bmpr2* KD mice, including intestinal hyperplasia (Figure 3) and gastric adenoma (data not shown). In *Bmpr2* KD mice age 5 months and older, large solitary polyps emerged in both small and large intestines with variable appearance, ranging from pedunculated masses with stalks to sessile lumps attached to the submucosa by a broad base. In some areas of the lesions, epithelial cells formed irregular tubular cysts and distorted glands arranged around a central lumina (Figure 3A,C). Prominent mitotic figures and positive staining for mitotic marker Ki67 indicated hyperplasia (Figure 3C,E). In addition, dilated, thin-walled blood vessels, with evidence of thrombosis and extravasation, were often found near the luminal surface (Figure 3B,D).

BMP signaling through BMPR1A has been proposed to restrict intestinal stem cell renewal by suppressing the Wnt/β-catinin axis through regulation of the phosphoinositol-3-kinase (PI3K)/AKT pathway.[16] Consistent with this hypothesis, the epithelial hyperplasia in the *Bmpr2* KD mice was associated with increased activation of AKT (Figure 3F). These results indicate that BMP receptors, together with components of the PI3K and WNT pathways, constitute a signaling circuit that controls balanced GI epithelial progenitor cells. Disturbance of this local environment may also contribute to the development of abnormal vasculature.

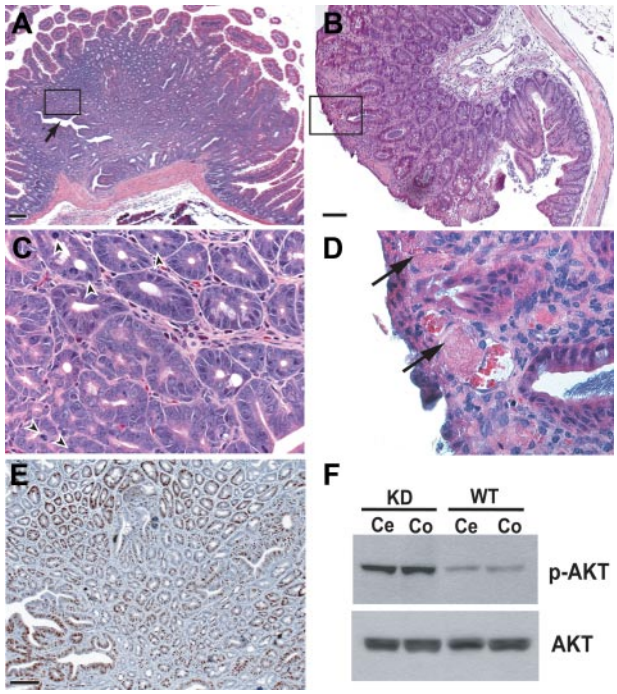

Figure 3. Intestinal polyposis in *Bmpr2*-deficient mice. Hamartoma-like polypoid mass formation in duodenum (A,C,E), and cecum (B,D) of *Bmpr2* KD mice. (C,D) Enlarged views of the boxed area in panels A and B, respectively. Arrow in panel A indicates disorganized epithelial glands, and arrowheads in panel C point to mitotic figures and distorted nuclear morphology. (E) Ki67 staining of adjacent serial sections. Bars = 100 μm. (F) Immunoblots of protein extracts from cecum (Ce) and colon (Co) of a *Bmpr2* KD mouse and its wild-type littermate using antibodies against phosphor-AKT and total AKT.

Deficient mural cell investment of the blood vessels from *Bmpr2* knockdown mice

Despite the apparent vascular malformation, pulmonary artery medial hypertrophy and neointima formation commonly found in PAH were not observed in *Bmpr2* KD mice. Accordingly, right ventricular systolic pressure was not elevated (Figure S1, available on the *Blood* website; see the Supplemental Materials link at the top of the online article). On the other hand, the muscular, preacinar pulmonary arteries associated with terminal bronchial in *Bmpr2* KD mice were markedly dilated. These vessels also exhibited disorganized adventitia and disproportionally thinner tunica media between the otherwise intact inner and outer elastic lamina (Figure 4A, top panel). A paucity of smooth muscle coverage in the media of pulmonary arteries was demonstrated by α-actin staining and morphometric measurement of media thickness (Figure 4A, middle panel, and Figure 4B). Similarly, small yet ectatic vessels in the submucosal layer of large intestine from *Bmpr2* KD mice exhibited regions that lack smooth muscle cells (Figure 4A, bottom panel). Such irregularity in the vessel wall may have contributed to the rupture and hemorrhage at focal areas subjected to chronic mechanical stress. Finally, expression of a marker for pericyte precursor, PDGFRβ, was markedly lower in lung protein extracts from *Bmpr2* KD mice, whereas endothelium-specific TIE2 expression did not change (Figure 4C). PDGFRβ autophosphorylation was not further repressed, indicating that disruption of a process independent of PDGF receptor activation may have caused the reduction in either pericyte recruitment to pulmonary vessels or expression of the receptor itself. Therefore, similar to ALK1[8] and endoglin,[17] BMPR2 plays a role in the establishment and maintenance of mural cell coverage on mature vessels.

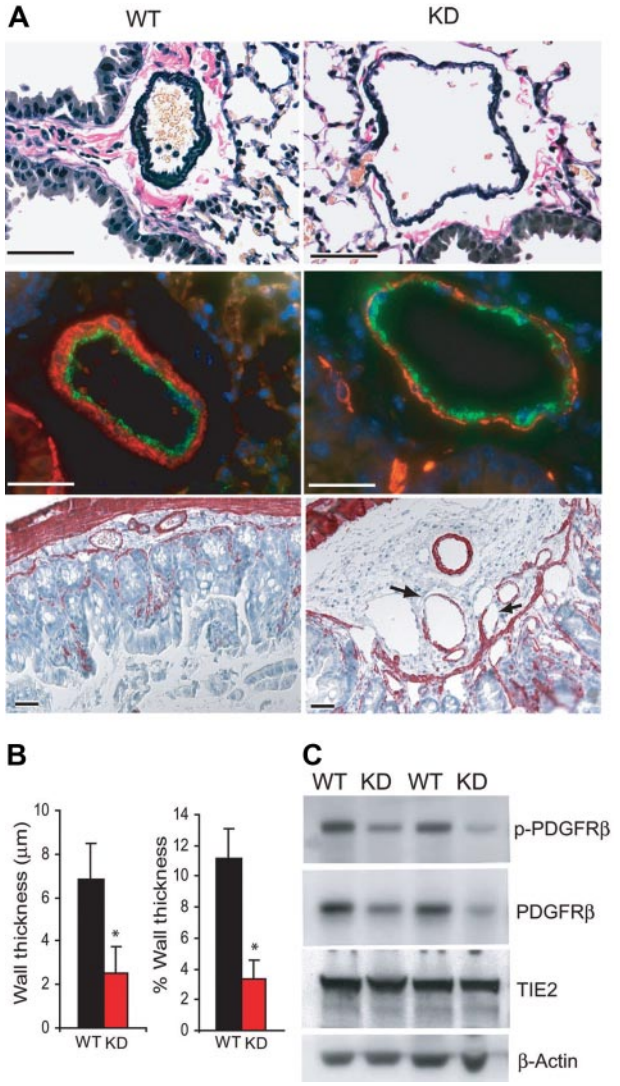

Figure 4. Defective mural cell coverage of blood vessels from *Bmpr2* KD mice. (A) (Top) Elastin-Van Gieson staining of pulmonary arteries from wild-type or *Bmpr2* KD mice. Note the rarified appearance of the tunica media. (Middle) Immunoflurescence staining of pulmonary arteries using anti-VWF, labeling endothelial cells, and anti-α-actin, labeling smooth muscle cells. (Bottom) Antismooth muscle α-actin immunohistochemistry of the large intestine. Arrows indicate areas missing SMCs. Bars = 50 μm. (B) Quantification of average wall thickness and wall thickness relative to external diameter of muscular, preacinar pulmonary arteries. Values are means plus or minus SD. *$P < .01$. (C) Immunoblots of lung extracts from 2 wild-type and 2 KD mice with the indicated antibodies.

Impaired angiogenesis of *Bmpr2*-deficient endothelial cells

To define the molecular and cellular basis for BMPR2-dependent vascular functions, we characterized the consequence of exogenous BMP signals in cultured primary lung endothelial cells (ECs). In ECs isolated from *Bmpr2* KD mice, the phosphorylation of SMAD1/5/8 in response to BMP4 was largely ablated (Figure 5A). Unlike BMP4 or other members of the BMP family, BMP9 and BMP10 were recently shown to have a distinct affinity to alternative type I (ALK1) and type II (BMPR2 plus ACVR2A) receptors.[18-20] Therefore, we investigated the response of primary ECs to BMP9. Not surprisingly, BMP9-stimulated Smad phosphorylation was only partially diminished in the *Bmpr2* KD cells (Figure 5A, bottom 2 panels), possibly reflecting a functional compensation by the ACVR2A-ALK1 complex. In normal ECs, the addition of BMP4 did not significantly affect cell proliferation (data not shown). However, it potently repressed the cell migration induced by sphingosine-1-phosphate (S1P) (Figure 5B), a PI3K/AKT-dependent event.[21] This repression correlated with reduced AKT activation by S1P in the presence of BMP4 or BMP9 (Figure 5C). Similarly, BMP4 treatment inhibited VEGF- and S1P-stimulated AKT activation in wild-type but not *Bmpr2* KD cells, and such differential response was evident, yet less pronounced, in the presence of serum (Figure 5D). Consistent with a positive effect of AKT on cell survival, BMP4 treatment increased EC apoptosis induced by serum deprivation, and this action appeared to depend on intact *Bmpr2* expression (Figure 5E). Therefore, as has been demonstrated in intestinal stem cells, the endothelial BMPR2 signaling can limit AKT activity, which is a critical mediator of angiogenesis.

To further evaluate the dependence of EC function on BMPR2, Matrigel plugs containing recombinant bFGF, either alone or together with BMP4, were implanted subcutaneously into the abdominal region of wild-type or *Bmpr2* KD mice (Figure 6). The degree of endothelial cell infiltration in bFGF-loaded gel plugs was similar regardless of the presence of BMP4 or host genotype despite considerable variation among individual animals. The number of cell-lined, red blood cell (RBC)–filled small vessels or tubular structures with lumen, however, was reduced in bFGF-loaded Matrigel implanted in *Bmpr2* KD mice. In addition, RBC-filled pools lacking cell lining, representing ruptured vessels, were more frequent in these plugs. The blood pooling was partially alleviated in BMP4-loaded gel isolated from the same animals. These results are in agreement with a role demonstrated previously

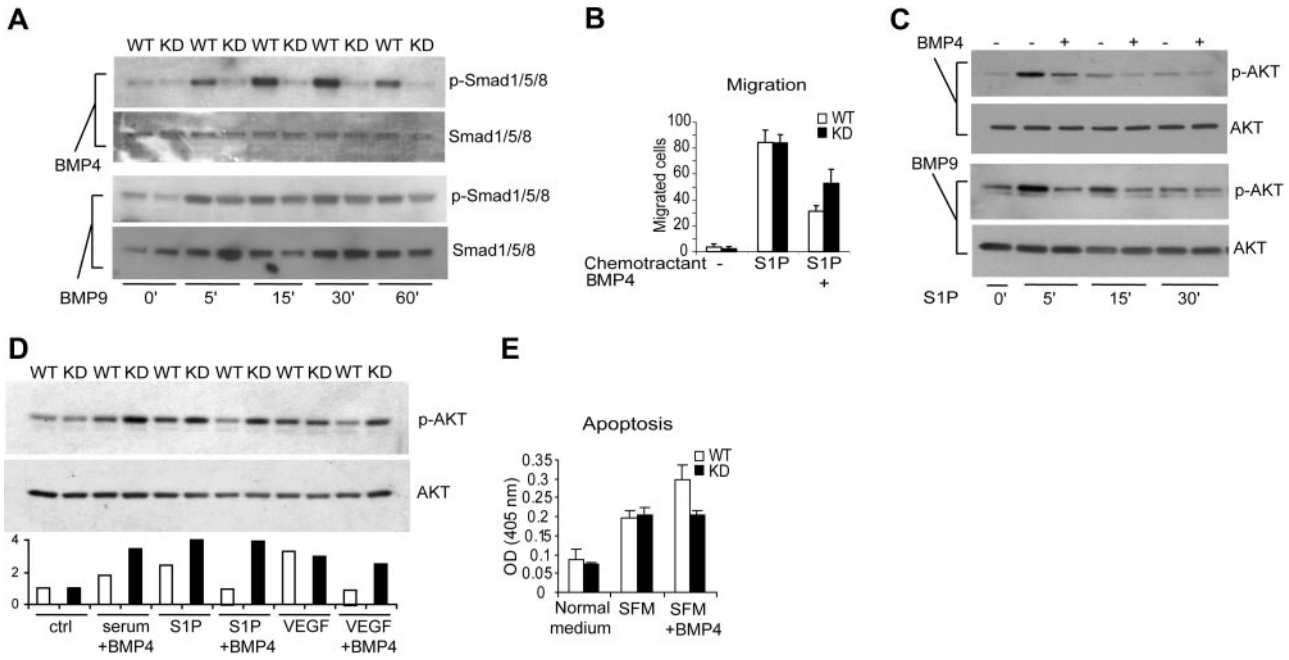

Figure 5. Dysregulated AKT activity in *Bmpr2* KD pulmonary vascular endothelial cells. (A) Characterization of SMAD-mediated signaling. Wild-type or *Bmpr2* KD cells were treated with 100 ng/mL BMP4 or BMP9 for the indicated time. Cell lysates were immunoblotted with antibodies against phosphorylated or total SMADs. (B) Chemotactic migration of endothelial cells toward sphingosine-1-phosphate (S1P). Cells were pretreated with 200 ng/mL BMP4 or vehicle control. Data represent results from 3 independent experiments. (C) Effect of BMP signaling on AKT activation. Wild-type ECs were stimulated with S1P for the indicated time in the presence or absence of 200 ng/mL BMP4 or BMP9. Cell lysates were immunoblotted with phospho-AKT and total AKT antibodies. (D) Effect of BMP4 on S1P-, serum-, and VEGF-stimulated serine phosphorylation of AKT in wild-type versus *Bmpr2* KD cells. The graph below the blot shows densitometry quantification of the phosphor-AKT levels normalized to total AKT. The open bars represent wild-type ECs whereas solid bars represent *Bmpr2* KD cells. (E) Potentiation of EC apoptosis by BMP4. Cells were incubated in normal medium with 10% serum or serum-free medium (SFM) for 24 hours, and DNA fragmentation index was determined by Cell Death Detection enzyme-linked immunosorbent assay (Roche). Values are means plus or minus SD.

for TGF-β and BMPs derived from bone extracts in modulating bFGF-induced neoangiogenesis[22] and suggest that signaling through BMPR2 is required for ordered capillary morphogenesis and establishment of stable vascular architecture.

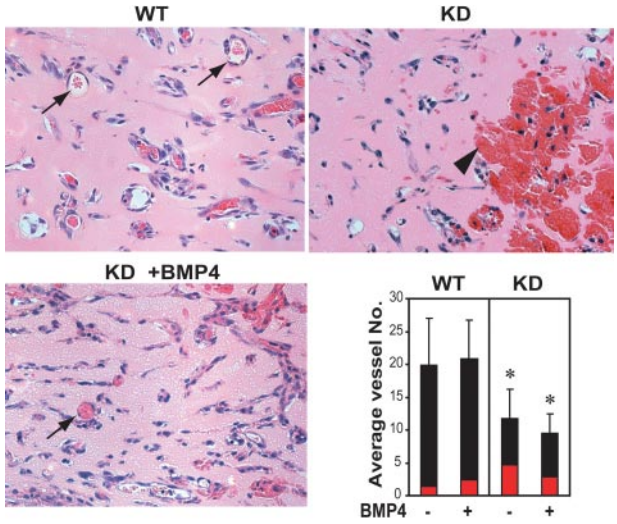

Figure 6. Abnormal angiogenesis in *Bmpr2* KD mice. Representative H&E-stained sections of Matrigel loaded with 200 ng/mL bFGF 7 days after implantation into the WT or *Bmpr2* KD mice are shown. Gel implants in WT mice mount robust neoangiogenesis and form well-defined, cell-lined vessels (arrows), whereas specimens from *Bmpr2* KD mice show increased hemorrhage and congestion (arrowhead), which were partially alleviated by the presence of exogenously supplied BMP4. Bar graph at lower right shows average number of RBC-containing vessels and tubular structures (black bar) or large blood pools (red bar) counted per × 400 microscopic field. Values are means plus or minus SD. *$P < .05$.

Aberrant regulation of vascular remodeling in *Bmpr2* knockdown mice

The unstable vasculature caused by defective BMP signaling, which probably predisposes to both the formation of HHT-like lesions and hemodynamic failure in the pulmonary circulation in PAH, prompted us to examine the expression of genes that regulate angiogenesis. Genome-wide transcriptional profiling was performed with ECs from *Bmpr2* KD and wild-type control mice. The cells used in this analysis were freshly isolated and purified without further culturing, thus allowing for an approximation of their physiologic state in vivo. By statistical filtering and selecting genes with previously documented involvement in vasculogenesis or angiogenesis, we established a panel of 25 genes to represent the transcriptional signature of *Bmpr2*-deficiencient lung endothelial cells (Figure 7A). Comparable transcriptional profiles were obtained for ECs from 2 independent *Bmpr2* knockdown mouse lines (Figure S2), suggesting that these changes were indeed due to deficiency in BMPR2 rather than off-target effect of the shRNA transgene.

A prominent feature of the *Bmpr2* KD signature panel is the downregulation of major determinants of vessel patterning and the maturation phase of angiogenesis. Among the few genes exhibiting dramatically reduced expression is *Sema3c,* encoding a class III semaphorin that regulates integrin activation and vascular remodeling.[23,24] Similarly, *Efnb1, Efnb2,* and *Epha4,* which provide repulsive navigational signals during blood vessels network patterning and arterial specification,[25] were concomitantly downregulated, along with *Jag2*, a ligand for notch that acts upstream of B-type ephrins.[26] Furthermore, endothelial production of a CXC chemokine *Cxcl12* (also known as *Sdf1*), was significantly decreased.

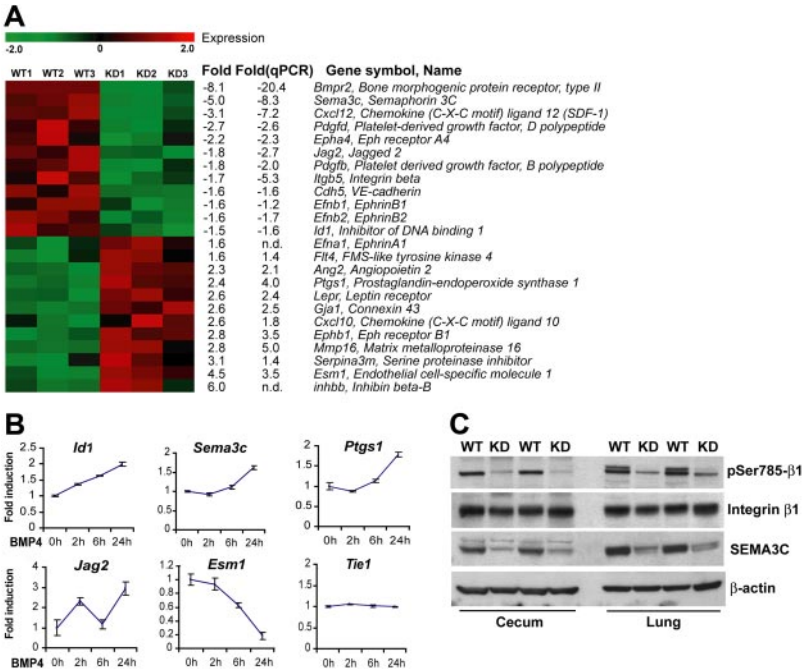

Figure 7. Identification of BMP-regulated genes in endothelial cells. (A) Hierarchical cluster diagram representing the expression pattern of 25 filtered genes with known angiogenic functions in endothelial cell isolations from wild-type and *Bmpr2* KD mice. Each row represents one gene and each column one independent cell preparation. Fold changes of expression evaluated in both GeneChip and quantitative RT-PCR analyses are indicated. Negative value denotes downregulation in the KD sample; n.d., not determined. (B) Real-time RT-PCR analyses of selected genes in cultured mouse lung endothelial cells treated with 100 ng/mL BMP4 for the indicated time. Values are means plus or minus SD. (C) Immunoblot detection of total or phosphor-Ser785 integrin β1 and SEMA3C in the lung and cecum from WT or KD littermates. Detection of β-actin in the same blot indicates equal loading.

Autocrine signaling through its receptor, CXCR4, is required for endothelial cell branching morphogenesis and organ-specific artery formation in the gut by remodeling primitive vessels.[27,28] Conversely, angiopoietin 2, a TIE2 antagonist primarily released by ECs that potently destabilizes quiescent endothelial monolayers,[29] was upregulated. Collectively, the distinct gene expression profile of *Bmpr2*-deficient endothelial cells indicates that BMP receptor signaling maintains a transcription program that controls vascular remodeling. This notion was reinforced by the finding that BMP4 treatment of wild-type ECs altered the expression of genes that were not previously recognized as BMP targets but showed deregulation in *Bmpr2* KD ECs (Figure 6B). Thus, the expression of *Sema3c* and *Jag2* was induced, along with known BMP downstream targets *Id1, Smad6,* and *Smad7* (Figure S2). By contrast, *Tie1* expression was not affected.

Because class III semaphorins are linked to regulation of integrin activation,[23,24] we evaluated the phosphorylation of Ser785 on integrin β1, which modifies its activity in cell adhesion and migration.[30] As shown in Figure 6C, the levels of serine phosphorylation on integrin β1, representing an activated state, were dramatically lower in both lung and intestinal tissues from *Bmpr2* KD mice, concomitant with a diminished SEMA3C protein expression. These results suggest that attenuation of BMP signals leads to disordered vessel assembly and stabilization, at least in part due to disturbed fine-tuning of integrin function by semaphorins.

Discussion

The establishment and maintenance of a mature, stable vasculature requires dynamic regulation of cell-cell and cell-matrix interactions. In this report, we demonstrate that BMP receptor signaling plays an indispensable role in such regulation. This function intricately depends on the receptor expression, consistent with the haploinsufficiency phenotype associated with other members of this pathway.[31-33] Our results illustrate the utility of a hypomorphic epi-allele series to uncover novel dosage-sensitive gene functions not revealed by conventional knockout approaches. RNAi in mice thus provides a powerful platform to analyze genes that are required for a diverse range of biologic processes.

Compromised vessel integrity and abdominal hemorrhage have been reported in mouse embryos with conditional *Bmpr1a*-null mutation.[10] A fraction of these embryos develop primitive vascular plexus but display dilated vessels with abnormal branching and disruption of vascular smooth-muscle cell (VSMC)–EC interactions. We found that RNAi knockdown of *Bmpr2* correlated with diminished PDGFRβ expression, presumably reflecting insufficient recruitment of mural cells. In addition, both *Pdgfb* and *Pdgfd* were downregulated in *Bmpr2*-deficient ECs, indicating an intrinsic defect in ECs, which direct the recruitment of mural cell precursors by secreting PDGF ligands.[34] Alternatively, the disproportional VSMC coverage may represent abnormal control over vessel caliber. This was suggested by the dilation of great vessels in developing chick embryos misexpressing SMAD7 regardless of the presence of VSMC, which is reversed by constitutively active BMP receptors.[35]

Endothelial dysfunction is central to the development of occlusive vasculopathy in PAH. Under pathogenic conditions, quiescent ECs initiate excessive growth and neoangiogenesis. In addition, unbalanced production of vasoactive mediators and paracrine growth factors by ECs facilitates changes in the contractile and proliferative responses of smooth-muscle cells. It is not clear whether loss of VSMC growth suppression by BMPs leads to lumen occlusion,[36,37] and the receptor appears to be more predominantly present on pulmonary ECs.[38] Furthermore, muscularization of the arterioles alone is also not sufficient to explain severe and progressive PAH. The disease is marked by plexiform/glomeruloid and angiomatoid endothelial lesions formed by an angioproliferative process combined with obliteration, or "pruning," of blocked arteriolar trees.[39] Similar processes may underlie the pathophysiology of HHT, because the hemorrhagic vascular malformations in *Bmpr2*-deficient mice resemble those in HHT mouse models with haploinsufficiency of EC-restricted *Alk1*[40] or *Eng*.[41] Consistent with this hypothesis, at least 2 BMP family ligands, BMP9 and BMP10, are capable of signaling through a receptor complex formed by

ALK1 and BMPR2.[18-20] In this study, we have provided additional evidence that this pathway regulates endothelial-cell migration that is dependent on the full function of BMPR2 despite the possible receptor redundancy. Given the clinical association between HHT and PAH,[14] the converging signals transmitted by BMPR2 and ALK1 may play redundant roles in establishing appropriate vessel connectivity and structural integrity. The disturbance of BMP signaling probably predisposes to injury of fragile vascular beds, such as in lung and intestinal mucosa, from focal hemodynamic and mechanical stress. The nature and duration of additional insults apparently dictate the spectrum of pathologic changes associated with PAH or HHT. Nonetheless, our studies did not exclude the possibility that BMP pathways regulate vascular function indirectly through cell lineages other than the endothelium. BMP-activated expression of Id proteins has been shown to facilitate the mobilization of bone marrow–derived endothelial progenitor cells.[42] Similarly, endoglin plays a crucial role in mononuclear cell–mediated revascularization following injury.[43] These finding suggest that defective repair of endothelial damage due to progenitor cell dysfunction might also contribute to the pathogenesis of HHT and PAH.

Considering the role of BMP signaling in tissue homeostasis, it is not coincidental that both vascular malformation and epithelial hyperplasia emerged in the GI tract of the *Bmpr2* KD mice. Hereditary diseases linked to perturbed TGF-β/BMP pathways, including PAH, HHT, and juvenile polyposis syndrome, share clinical features.[44] It is therefore tempting to speculate that common pathways may maintain the quiescent state of distinct cells. We found increased AKT activation in the intestine and growth factor–treated endothelial cells from *Bmpr2* KD mice, which may contribute to both polyposis and uncontrolled angiogenic activity. Indeed, exposure of epithelial cells to BMP2 results in decreased PTEN protein degradation,[45] and endothelial-specific *Pten* knockout mice show vascular defects similar to BMP receptor mutants,[46] lending support to the crosstalk between the 2 pathways during vascular development.

We have begun to further dissect the molecular effectors of the BMP pathway that regulate angiogenesis by transcriptional profiling of *Bmpr2*-deficient endothelial cells. Overall, the gene expression pattern implies that these cells have reverted to a destabilized, more plastic state. Analyses of BMPR2-dependent transcription also revealed coordinated regulation of neural guidance molecules implicated in vascular remodeling. For example, we observed a downregulation of *Efnb2* in *Bmpr2*-deficient endothelial cells. A similar change was reported in *Alk1*-deficient mice, which probably contributes to arteriovenous malformation through disruption of distinct arterial and venous identity.[9] Most significantly, the BMPR2-dependent expression of a class III semaphorin, and the defective β1 integrin activation that correlates with the loss of SEMA3C autocrine signaling in *Bmpr2* KD mice, strongly supports a role for such molecules downstream of BMPs that provide pathfinding cues to both endothelial and neuronal morphogenesis through modulation of cell adhesion or establishing zones of exclusion for cell migration.[23,47] In the absence of proper positional guidance, vascular malformation ensues. Attesting to the significance of semaphorin in BMP signaling, *Sema3a*-null mice manifest pronounced and selective hypertrophy of the right ventricle of the heart and dilation of the right atrium, a hallmark of pulmonary hypertension, although such causal relationship has not been fully established.[48] Similar to *Bmp4,*[49] *Bmpr1a,*[10] or *Bmpr2,*[50] *Sema3c* and its receptor, plexin D, are required for proper separation of the cardiac outflow tract and vessel patterning.[51,52] Further investigation on the interactions between BMP, semaphorin, and integrin pathways should shed new light on their involvement in as yet poorly characterized pulmonary vascular diseases.

Acknowledgments

We are grateful to H. Su, Q. Fang, J. Markovitz, W. Marston, N. Avitahl-Curtis, O. Tarnavski, M. Constant, M. Goetschkes, T. Troung, and A. Ho for technical assistance. We also thank Dr P. Oh for critical reading of the manuscript.

Authorship

Contribution: D.L., J.W., B.K., and M.M. performed research and analyzed results; X.M., R.V., and Y.L. assisted in data analyses; D.L. and E.L. conceived the project; and D.L. wrote the paper.

Conflict-of-interest disclosure: The authors declare no competing financial interests.

Correspondence: Dong Liu, Novartis Institutes for Biomedical Research, 250 Massachusetts Ave, 5C-344, Cambridge, MA 02139; e-mail: dong.liu@novartis.com.

References

1. Feng XH, Derynck R. Specificity and versatility in TGF-β signaling through Smads. Annu Rev Cell Dev Biol. 2005;21:659-693.
2. Valdimarsdottir G, Goumans MJ, Rosendahl A, et al. Stimulation of Id1 expression by bone morphogenetic protein is sufficient and necessary for bone morphogenetic protein-induced activation of endothelial cells. Circulation. 2002;106:2263-2270.
3. Langenfeld EM, Langenfeld J. Bone morphogenetic protein-2 stimulates angiogenesis in developing tumors. Mol Cancer Res. 2004;2:141-149.
4. Winnier G, Blessing M, Labosky PA, Hogan BL. Bone morphogenetic protein-4 is required for mesoderm formation and patterning in the mouse. Genes Dev. 1995;9:2105-2116.
5. Chang H, Huylebroeck D, Verschueren K, Guo Q, Matzuk MM, Zwijsen A. Smad5 knockout mice die at mid-gestation due to multiple embryonic and extraembryonic defects. Development. 1999;126:1631-1642.
6. Yang X, Castilla LH, Xu X, et al. Angiogenesis defects and mesenchymal apoptosis in mice lacking SMAD5. Development. 1999;126:1571-1580.
7. Bourdeau A, Dumont DJ, Letarte M. A murine model of hereditary hemorrhagic telangiectasia. J Clin Invest. 1999;104:1343-1351.
8. Oh SP, Seki T, Goss KA, et al. Activin receptor-like kinase 1 modulates transforming growth factor-β1 signaling in the regulation of angiogenesis. Proc Natl Acad Sci U S A. 2000;97:2626-2631.
9. Urness LD, Sorensen LK, Li DY. Arteriovenous malformations in mice lacking activin receptor-like kinase-1. Nat Genet. 2000;26:328-331.
10. Park C, Lavine K, Mishina Y, Deng CX, Ornitz DM, Choi K. Bone morphogenetic protein receptor 1A signaling is dispensable for hematopoietic development but essential for vessel and atrioventricular endocardial cushion formation. Development. 2006;133:3473-3484.
11. Lane KB, Machado RD, Pauciulo MW, et al. Heterozygous germline mutations in BMPR2, encoding a TGF-β receptor, cause familial primary pulmonary hypertension. The International PPH Consortium. Nat Genet. 2000;26:81-84.
12. Machado RD, Aldred MA, James V, et al. Mutations of the TGF-β type II receptor BMPR2 in pulmonary arterial hypertension. Hum Mutat. 2006;27:121-132.
13. Johnson DW, Berg JN, Baldwin MA, et al. Mutations in the activin receptor-like kinase 1 gene in hereditary haemorrhagic telangiectasia type 2. Nat Genet. 1996;13:189-195.
14. Trembath RC, Thomson JR, Machado RD, et al. Clinical and molecular genetic features of pulmonary hypertension in patients with hereditary hemorrhagic telangiectasia. N Engl J Med. 2001;345:325-334.

15. Beppu H, Kawabata M, Hamamoto T, et al. BMP type II receptor is required for gastrulation and early development of mouse embryos. Dev Biol. 2000;221:249-258.
16. He XC, Zhang J, Tong WG, et al. BMP signaling inhibits intestinal stem cell self-renewal through suppression of Wnt-β-catenin signaling. Nat Genet. 2004;36:1117-1121.
17. Sorensen LK, Brooke BS, Li DY, Urness LD. Loss of distinct arterial and venous boundaries in mice lacking endoglin, a vascular-specific TGFβ coreceptor. Dev Biol. 2003;261:235-250.
18. Brown MA, Zhao Q, Baker KA, et al. Crystal structure of BMP-9 and functional interactions with pro-region and receptors. J Biol Chem. 2005; 280:25111-25118.
19. David L, Mallet C, Mazerbourg S, Feige JJ, Bailly S. Identification of BMP9 and BMP10 as functional activators of the orphan activin receptor-like kinase 1 (ALK1) in endothelial cells. Blood. 2007; 109:1953-1961.
20. Scharpfenecker M, van Dinther M, Liu Z, et al. BMP-9 signals via ALK1 and inhibits bFGF-induced endothelial cell proliferation and VEGF-stimulated angiogenesis. J Cell Sci. 2007;120: 964-72.
21. Lee MJ, Thangada S, Paik JH, et al. Akt-mediated phosphorylation of the G protein-coupled receptor EDG-1 is required for endothelial cell chemotaxis. Mol Cell. 2001;8:693-704.
22. Roedersheimer M, West J, Huffer W, Harral J, Benedict J. A bone-derived mixture of TGFβ-superfamily members forms a more mature vascular network than bFGF or TGF-β2 in vivo. Angiogenesis. 2005;8:327-338.
23. Serini G, Valdembri D, Zanivan S, et al. Class 3 semaphorins control vascular morphogenesis by inhibiting integrin function. Nature. 2003;424:391-397.
24. Banu N, Teichman J, Dunlap-Brown M, Villegas G, Tufro A. Semaphorin 3C regulates endothelial cell function by increasing integrin activity. FASEB J. 2006;20:2150-2152.
25. Poliakov A, Cotrina M, Wilkinson DG. Diverse roles of eph receptors and ephrins in the regulation of cell migration and tissue assembly. Dev Cell. 2004;7:465-480.
26. Fischer A, Schumacher N, Maier M, Sendtner M, Gessler M. The Notch target genes Hey1 and Hey2 are required for embryonic vascular development. Genes Dev. 2004;18:901-911.
27. Ara T, Tokoyoda K, Okamoto R, Koni PA, Nagasawa T. The role of CXCL12 in the organ-specific process of artery formation. Blood. 2005;105: 3155-3161.
28. Salvucci O, Yao L, Villalba S, Sajewicz A, Pittaluga S, Tosato G. Regulation of endothelial cell branching morphogenesis by endogenous chemokine stromal-derived factor-1. Blood. 2002;99: 2703-2711.
29. Scharpfenecker M, Fiedler U, Reiss Y, Augustin HG. The Tie-2 ligand angiopoietin-2 destabilizes quiescent endothelium through an internal autocrine loop mechanism. J Cell Sci. 2005;118:771-780.
30. Mulrooney JP, Hong T, Grabel LB. Serine 785 phosphorylation of the β1 cytoplasmic domain modulates β1A-integrin-dependent functions. J Cell Sci. 2001;114:2525-2533.
31. Shore EM, Xu M, Feldman GJ, Fenstermacher DA, Brown MA, Kaplan FS. A recurrent mutation in the BMP type I receptor ACVR1 causes inherited and sporadic fibrodysplasia ossificans progressiva. Nat Genet. 2006;38:525-527.
32. Dunn NR, Winnier GE, Hargett LK, Schrick JJ, Fogo AB, Hogan BL. Haploinsufficient phenotypes in Bmp4 heterozygous null mice and modification by mutations in Gli3 and Alx4. Dev Biol. 1997;188:235-247.
33. Takaku K, Oshima M, Miyoshi H, Matsui M, Seldin MF, Taketo MM. Intestinal tumorigenesis in compound mutant mice of both Dpc4 (Smad4) and Apc genes. Cell. 1998;92:645-656.
34. Hirschi KK, Rohovsky SA, D'Amore PA. PDGF, TGF-β, and heterotypic cell-cell interactions mediate endothelial cell-induced recruitment of 10T1/2 cells and their differentiation to a smooth muscle fate. J Cell Biol. 1998;141:805-814.
35. Vargesson N, Laufer E. Smad7 misexpression during embryonic angiogenesis causes vascular dilation and malformations independently of vascular smooth muscle cell function. Dev Biol. 2001;240:499-516.
36. Morrell NW, Yang X, Upton PD, et al. Altered growth responses of pulmonary artery smooth muscle cells from patients with primary pulmonary hypertension to transforming growth factor-β1 and bone morphogenetic proteins. Circulation. 2001;104:790-795.
37. Frank DB, Abtahi A, Yamaguchi DJ, et al. Bone morphogenetic protein 4 promotes pulmonary vascular remodeling in hypoxic pulmonary hypertension. Circ Res. 2005;97:496-504.
38. Atkinson C, Stewart S, Upton PD, et al. Primary pulmonary hypertension is associated with reduced pulmonary vascular expression of type II bone morphogenetic protein receptor. Circulation. 2002;105:1672-1678.
39. Voelkel NF, Cool C. Pathology of pulmonary hypertension. Cardiol Clin. 2004;22:343-351, v.
40. Srinivasan S, Hanes MA, Dickens T, et al. A mouse model for hereditary hemorrhagic telangiectasia (HHT) type 2. Hum Mol Genet. 2003;12: 473-482.
41. Torsney E, Charlton R, Diamond AG, Burn J, Soames JV, Arthur HM. Mouse model for hereditary hemorrhagic telangiectasia has a generalized vascular abnormality. Circulation. 2003;107: 1653-1657.
42. Lyden D, Hattori K, Dias S, et al. Impaired recruitment of bone-marrow-derived endothelial and hematopoietic precursor cells blocks tumor angiogenesis and growth. Nat Med. 2001;7:1194-1201.
43. van Laake LW, van den Driesche S, Post S, et al. Endoglin has a crucial role in blood cell-mediated vascular repair. Circulation. 2006;114:2288-2297.
44. Waite KA, Eng C. From developmental disorder to heritable cancer: it's all in the BMP/TGF-β family. Nat Rev Genet. 2003;4:763-773.
45. Waite KA, Eng C. BMP2 exposure results in decreased PTEN protein degradation and increased PTEN levels. Hum Mol Genet. 2003;12:679-684.
46. Hamada K, Sasaki T, Koni PA, et al. The PTEN/PI3K pathway governs normal vascular development and tumor angiogenesis. Genes Dev. 2005; 19:2054-2065.
47. Shoji W, Isogai S, Sato-Maeda M, Obinata M, Kuwada JY. Semaphorin3a1 regulates angioblast migration and vascular development in zebrafish embryos. Development. 2003;130:3227-3236.
48. Behar O, Golden JA, Mashimo H, Schoen FJ, Fishman MC. Semaphorin III is needed for normal patterning and growth of nerves, bones and heart. Nature. 1996;383:525-528.
49. Liu W, Selever J, Wang D, et al. Bmp4 signaling is required for outflow-tract septation and branchial-arch artery remodeling. Proc Natl Acad Sci U S A. 2004;101:4489-4494.
50. Délot EC, Bahamonde ME, Zhao M, Lyons KM. BMP signaling is required for septation of the outflow tract of the mammalian heart. Development. 2003;130:209-220.
51. Feiner L, Webber AL, Brown CB, et al. Targeted disruption of semaphorin 3C leads to persistent truncus arteriosus and aortic arch interruption. Development. 2001;128:3061-3070.
52. Gitler AD, Lu MM, Epstein JA. PlexinD1 and semaphorin signaling are required in endothelial cells for cardiovascular development. Dev Cell. 2004;7:107-116.